FABIAN MURALTER

Oxidative Chemical Vapor Deposition of a Conducting Polymer Film on Nanostructured Surfaces for Piezoresistive Sensor Applications

From Vapor Deposition to Piezoresistivity

MARSHALL PLAN SCHOLARSHIP PAPER

September 30th, 2019 – March 2nd, 2020

Host Institution: Drexel University

Home Institution: Graz University of Technology

Supervisors:

PROF. KENNETH K. LAU, PHD
Department of Chemical and Biological Engineering
Drexel University

ASSOC.-PROF. DR. ANNA MARIA COCLITE
Institute of Solid State Physics
Graz University of Technology

Graz, April 30, 2020

Contents

Abstract

In this study, a novel, fully polymeric setup for piezoresistive sensing was prepared and tested. For this setup, a monolayer of polystyrene (PS) nanospheres (with a diameter of ~580 nm) was assembled on a flexible polyethylene naphthalate (PEN) substrate. Subsequently, a thin layer (~50-100 nm) of poly(3,4-ethylenedioxythiophene) (PEDOT) was deposited conformally around the spheres via oxidative chemical vapor deposition (oCVD). Two nickel top-contacts with a separation of 0.5 mm were used to characterize the individual samples. Voltage-current characteristics and direct resistance measurements were performed to test the electrical properties of the samples in their unstrained state and their piezoresistive response during bending. The substrate temperature and deposited thickness during oCVD were used as parameters to alter the properties of the PEDOT thin film, with increased substrate temperature and thickness leading to samples exhibiting lower intrinsic resistance. An estimation of the conductivity of the samples prepared yielded values of up to tens of S cm^{-1}. Intrinsically, with the setup used, the oCVD-PEDOT layer is chlorine-doped. Subsequent dopant exchange by putting the samples in 0.5 M sulfuric acid decreased their resistance by ~1/3. Regarding the piezoresistive properties of the devices prepared, lower intrinsic resistance and the acid treatment performed enhanced the response of the samples. Thus, in the range of parameters investigated, acid treatment, higher substrate temperatures and thickness yielded samples with increased response. As a result, gauge factors as high as 11.4 could be achieved. These results offer a promising basis for further investigations in a novel approach.

Introduction

The piezoresistive effect is broadly used in various devices such as transducers, accelerometers, piezo-FETs, etc. and most prominently in sensors.[1] Its basis is a change in resistance caused by a deformation of a material (i.e., strain). Thus, bending, pressure or stress acting on a piezoresistive material can be measured as a change in resistance as a function of strain. In this work, the objective of strain sensing with a novel, fully polymeric setup is proposed to serve as a basis, from which further possible applications can be derived in the future. Up to now, such materials are mostly silicon-based or involve other inorganic rigid solids. Their rigidity, however, is disadvantageous, if large strains and/or small pressures are of interest. To overcome this limitation, hybrid setups mainly consisting of inorganic nanostructures supported by flexible polymers have been investigated. In the last decade, strain sensors based on solution-processed piezoresistive polymer films (e.g., PEDOT:polystyrene sulfonate or PSS) have also been developed.[2–4] However, these setups exhibit lower sensitivity than their inorganic counterparts do. Recently, the integration of nanostructures into the polymers towards a new generation of strain sensors has been reported.[1,4,5] This was reported to enhance the sensitivity by orders of magnitude. Moreover, the high mechanical flexibility typical for polymers is crucial for the application in various groundbreaking and growing fields such as wearable electronics. As the size of the nanostructures used is in the order of tens to hundreds of nanometers, the prospect in the present project is to use polymeric nanostructures of similar sizes. Furthermore, the piezoresistivity of PEDOT:PSS was reported to depend on the sizes of PEDOT- and PSS-rich domains, when PEDOT is doped with solid state PSS.[3,4] The present project aims to investigate and utilize this fact by conformal deposition of PEDOT thin films of different thicknesses around PS nanospheres assembled on the surface of a flexible substrate. Monolayers of PS nanospheres deposited onto flexible substrates serve as a basis for the proposed structure. The data in the literature suggests that the quality of and even the ability to deposit such PS monolayers strongly depends on the quality and impurities in the PS nanosphere suspension that is used.[6] The goal is to reproducibly deposit such uniform monolayers over large areas. Simple drop casting, spin coating and doctor blading were proposed, fulfilling this task to a varying extent. However, deposition of the PS beads onto the air-water interface and subsequent pick-up onto a substrate appears to yield the most convincing and reproducible results.[6,7]

Onto the monolayer of PS nanospheres, a PEDOT thin film will be deposited conformally around the nanostructure. Oxidative chemical vapor deposition (oCVD) specifically meets this need for conformality without damaging the substrate and with the advantage of vapor-phase processing (i.e., no swelling of PS during deposition in solutions). Acid treatment post-oCVD was shown to lead to a dopant exchange and, thus, altered film properties.[8] The described acid treatment of the entire structure also leads to a sulfonation/doping of the surfaces of the PS nanospheres.[9] Therefore, such acid treatment can be utilized to further understand the role of the PEDOT-PS interfaces on the piezoresistive effect of the resulting structure. A contribution of the doped aromatic units on the surfaces of the PS spheres to the conduction mechanisms in the material is assumed. Furthermore, parameters such as the substrate temperature during oCVD, or the flow rates of the individual chemical precursors used were shown to lead to different properties (e.g., conductivity) of the resulting PEDOT thin films.[10]

The piezoresistive response of such samples, when strained, can be estimated by measuring voltage-current characteristics during bending (e.g., cf. Latessa et al.[3]). By choosing the right electrode material (i.e., matching work functions; ohmic contact), resistance measurements between two top-contacts deposited at a well-defined spacing suffice. Therefore, from calculating the strain via bending radii, the response of the samples is estimated as the percentage of the resistance change during bending and normalizing the value by the resistance value measured in the unstrained state. The response of the individual samples is investigated as a function of substrate temperature during oCVD, PEDOT thickness and acid treatment.

Methods

Sample preparation

Silicon wafers (University Wafer) were used as test substrates for the deposition of polystyrene (PS) nanospheres and poly(3,4-ethylenedioxythiophene) (PEDOT) thin films. Polyethylene naphthalate (PEN) films (thickness 0.125 μm, Goodfellow) were used as substrates for the final test devices.

Various PEDOT thin films were synthesized by oxidative chemical vapor deposition (oCVD) in a custom-built reactor described by Smolin & Lau et al.[11,12] 3,4-Ethylenedioxythiophene (EDOT, 97%, Sigma-Aldrich) and vanadium oxytrichloride ($VOCl_3$, 99%, Sigma-Aldrich) were used as-received, and placed in separate glass jars as the liquid monomer and oxidant

sources, respectively. The glass jar of EDOT was heated to 90°C, whereas $VOCl_3$ was kept at room temperature. For all the depositions described, both flow rates were set to 1 sccm (standard cubic centimeter per min) via individual low-flow precision metering valves (Swagelok). Nitrogen (1 sccm each) was used as an inert carrier gas to promote transport of the monomer and oxidant into the reaction chamber through individual gas lines. The pressure in the reaction chamber was monitored and controlled by a pressure controller in a feedback loop with a downstream throttle valve and a pressure transducer (MKS Instruments). During the depositions, the pressure was kept constant in the range of 100-400 mTorr. For the described depositions, the substrate stage was held at constant temperatures between 40 and 80 °C. The depositions were carried out for 30 or 60 min to achieve samples of different film thickness at a certain substrate temperature and pressure.

Polystyrene (PS) nanospheres are deposited onto the respective substrates from various suspensions. Commercially available dispersions of PS beads in water were purchased from Polysciences, Inc. (1 μm; 2.5 wt.-%, carboxylate-functionalized and plain) and from Microparticles GmbH (0.757 μm; 5 wt.-%). Suspensions in ethanol (EtOH), methanol (MeOH) with and without addition of a surfactant (Triton X-100, Sigma-Aldrich) were prepared from the commercial dispersions (cf. Hulteen et al.[13], Trujillo et al.[14]). The methods of drop casting, spin coating and doctor blading were tested for the deposition of monolayers of PS beads from such suspensions. Furthermore, the assembly of a monolayer at an air-water interface was tested with suspensions of 1:1 volume ratio of EtOH and the as-received H_2O-dispersions of PS beads (cf. Vogel et al.[7]). Another dispersion of PS beads in water (580 nm; 5 wt.-%) prepared by surfactant-free emulsion polymerization was kindly provided by Prof. Vogel's group in Erlangen, Germany. This dispersion was used for the assembly of monolayers at the air-water interface as reported in Vogel et al.[7] The PS beads were added to the air-water interface in a glass beaker (8 cm diameter, 4.5 cm height) by dropping several microliters of the PS-H_2O:EtOH dispersion onto the dry end of a plasma-cleaned microscopy glass slide partially immersed in the water and tilted to ~45°. All the water used in these experiments was provided by a Milli-Q water purification station yielding deionized H_2O with a resistance value of 18.2 MΩ cm. The EtOH used (200 Proof, Decon Laboratories, Inc.) had a purity of 99.2%. All the substrates were plasma-cleaned under an air-atmosphere in a Harrick PDS-001 plasma cleaner for 10 min at 30 W.

Acid treatment was performed by placing the samples (PEDOT on PS on PEN) in a H_2SO_4 solution. For this purpose, concentrated H_2SO_4 (Sigma-Aldrich) was diluted to a 0.5 M solution with MiliQ-water.

The deposition of Ni top-contacts was performed in a Thermionics VE 90 thermal evaporator with a contact mask creating a spacing of 0.5 mm between the two contacts. A quartz crystal microbalance (QMB) was used to monitor the Ni growth rate to achieve a target film thickness of (50 ± 2) nm.

Investigation

The individual substeps in the experimental procedure are monitored by investigating the molecular nature of the thin films by Fourier-transform infrared spectroscopy (FTIR) and the structure of the assembled setup by optical and scanning electron microscopy (SEM).

Fourier-transform infrared spectroscopy (FTIR) measurements were performed on a Thermo Nicolet 6700 spectrometer in transmission mode. The spectra were collected in the wavenumber range 400–4000 cm^{-1} at a resolution of 4 cm^{-1} using a DTGS detector.

Scanning electron microscopy (SEM) was performed on a Zeiss Supra 50VP scanning electron microscope with an accelerating voltage of 5 kV. All the presented images were recorded at a working distance of ~11 mm. The samples were sputtered with Pt for 40 s before SEM analysis.

Voltage-current characteristics were measured on a Gamry Reference 600 system in the linear sweep voltammetry mode. The ohmic behavior of all the samples investigated was confirmed by the linear voltage-current characteristics and utilized so that further measurements could be performed on a Fluke 112 multimeter, directly evaluating the corresponding resistance values. Two different methods were used to connect the Ni contacts to the measurement device: crocodile clips or test leads. Both are used with a piece of aluminum foil in between to prevent the ultrathin nickel contact film from being scratched. Strain was exerted on the devices via bending (longitudinal to the separation of the contacts). The corresponding strain ε (defined as the change in length normalized by the length of the unstrained device $\Delta l/l$) can be calculated via the bending radii r_b utilized and the substrate thickness t_{sub} (for $r_b \gg t_{sub}$). Tensile strain is given as a positive value, compressive strain as a negative one.

$$\varepsilon = \frac{\Delta l}{l} = \frac{t_{sub}/2}{r_b + t_{sub}/2} \approx \frac{t_{sub}/2}{r_b}$$

The bending experiments were performed at constant temperature (22°C) and relative humidity (40%). The final device setup, as assembled and when strained, is sketched in Figure 1.

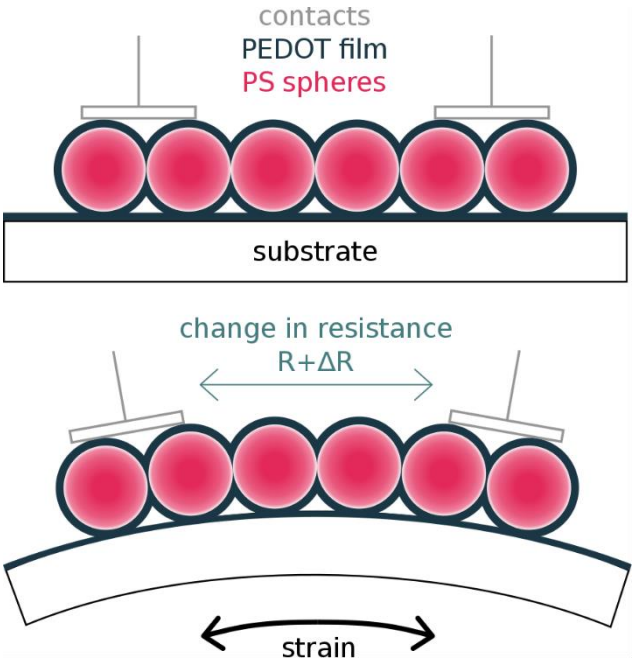

Figure 1: Sketch of the device structure proposed and tested for strain sensing, exhibiting a resistance value R as assembled/unstrained (top) and changing its resistance by ΔR when strained via bending (bottom)

Experimental, results and discussion

Assembly of monolayers of PS nanospheres

In the first step, various methods were tested for the deposition of a monolayer of polystyrene nanospheres on various surfaces, including silicon wafers and polyethylene naphthalate (PEN) substrates. The aim was to achieve monolayers over adequate areas (~cm^2) prepared with reasonable reproducibility. First, this should serve as a basis for the architecture used for testing and, subsequently, can ensure the potential for upscaling of the proposed methods.

At first, commercially available PS beads from Polysciences, Inc. were *drop casted* onto silicon wafers, as reported in Trujillo et al.[15]. Carboxylate-functionalized and plain beads (from Polysciences, Inc.) behaved similarly in the experiments described in the following. The as-received PS beads (2.5 wt% in water) were mixed 1:1 in volume with a solution of methanol and Triton X-100 (500:1 by volume). This solution was applied to the surface in drops of 1-10 µl and left to dry at ambient conditions until no liquid could be observed with the naked eye (~5 min). Subsequently, the substrates were dried for 30 min at 80 °C to remove any residual liquid. The drops smallest in volume (~1-2 µl) lead to the most promising results. However, optical and scanning electron microscopy revealed only very small areas (up to ~2 mm^2) of real monolayer coverage. Moreover, small regions showed coverages lower than a monolayer (i.e., de-wetted). The rest of the area covered by the applied drop (~1 cm in diameter in total) consisted of multilayers of PS nanospheres at the outermost parts (i.e., coffee ring effect) and in the middle of the drop . The SEM images shown in Figure 2 depict the structure of regions covered by a monolayer in such a way. Overall (see Figure 2 (a)), they exhibit a large number of lattice defects and dislocations with areas of hexagonally close-packed (hcp) nanospheres not larger than 10x10 spheres, areas of chaotic assembly of the beads (b) and regions of de-wetted structures with large areas (up to hundreds of micrometers) of bare substrate being visible between the deposited beads (c). The applied drops spread more effectively on plasma-cleaned substrates yielding regions of monolayer coverage of up to ~10 mm^2, still lower compared to other reports in the literature (e.g., 0.3 cm^2)[15]. The plasma-cleaning procedure applied (air, 30 W, 10 min) lowers the water contact angle on a silicon wafer from ~45° (uncleaned) to below 5° and, thus, also leads to better wetting of the applied drop. To promote spreading, different amounts of MeOH were added to the suspension prior to drop casting. However, more MeOH leads to immediate flow away from the center of the applied drop towards the edges of the substrate. Once the edges

were reached, the liquid flowed back towards the center of the applied drop causing very inhomogeneous PS layers. If the substrate was big enough (no flow back to the center of the applied drop), the coverage of PS spheres remained well below a monolayer, with large areas exhibiting no nanospheres at all. Similar results were obtained by using EtOH instead of MeOH with and without addition of the surfactant Triton X-100. As-received PEN substrates were observed to exhibit a water contact angle of ~60°, whereas it could be lowered to ~10° by plasma-cleaning. Thus, using the PEN substrates as received for the described experiments mostly lead to multilayer coverage. However, with the plasma-cleaned substrates, similar results as in the case of silicon wafers (described above) could be achieved.

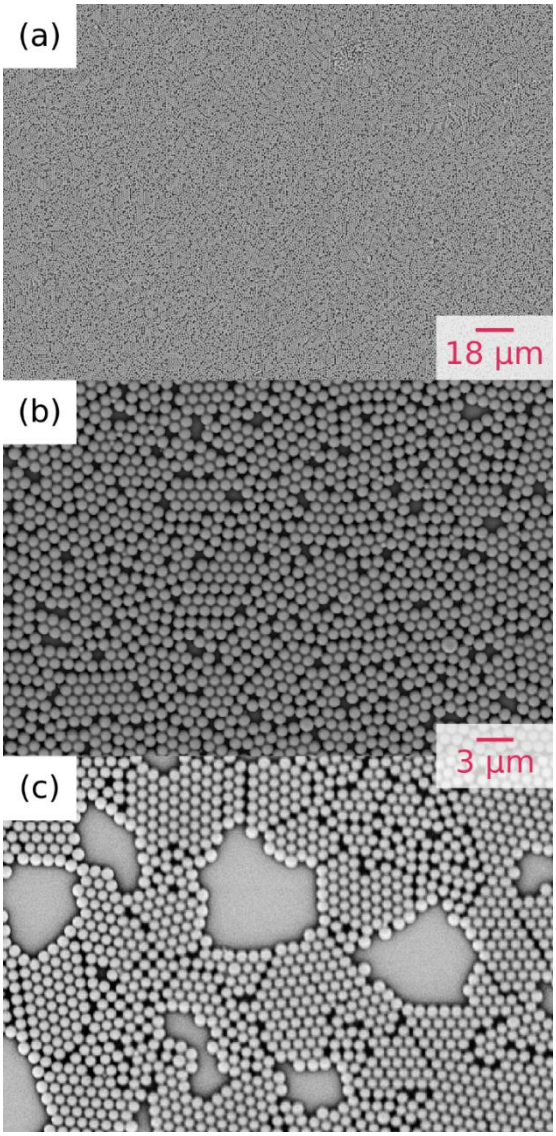

Figure 2: Scanning electron microscopy images of regions of monolayers of polystyrene nanospheres assembled on a silicon substrate by drop casting: (a) overview image of such an area, (b) area showing large numbers of defects, and (c) area showing de-wetted structures with voids between deposited spheres.

As a second technique, *spin coating* was applied to deposit a monolayer of PS beads onto the substrates from the suspensions previously described. Two cases were tested: High spin speeds (>200 rpm) that lead to the quick spreading/removal of the drop from the substrate and low spin speeds (<100 rpm) that move the drop on the wetted surface. Similar to the drop-casted samples, they were dried for 30 min at 80°C after spin coating to remove any residual liquid. In the first case, high spin speeds resulted in very low coverage. By waiting longer before starting spinning, the coverage could be increased, however, not to the extent of avoiding blank spots in the tens of micrometers in size. In the second case at low spin speeds, results similar to the best results obtained by drop casting could be obtained with regions of monolayer coverage in the order of 10 mm^2. An approach similar to Arutinov et al.[16] was applied to achieve regions with monolayer coverage over such areas. Specifically, increasing the spin speed from 80 rpm up to 1000 rpm by 100 rpm steps ca. every 2 min yielded the most promising results. The resulting PS monolayers exhibited similar structure (i.e., amounts of defects) as the ones prepared by drop casting, however, with a higher effort to obtain such results (e.g., need of a spin coater, setting up a routine).

In a further trial, *doctor blading* was evaluated as a technique to deposit a monolayer of PS beads on a substrate from the suspensions described above similar to Yang & Jiang[17]. A piece of silicon wafer was pinned down by two stripes of tape at either side of the substrate, also serving as a guard for the doctor blade. The drop was applied on one end of the bare region of the substrate and spread by pushing the blade across the substrate at a constant tilt angle and speed. Metal and plastic blades applying tilts between 10 and 90° were tested. Furthermore, different speeds (~0.1-10 cm/s) were tested, but with the disadvantage/unreliability of moving the blade manually. Slower speeds lead to more reproducible results. However, in all the conditions applied, inhomogeneous residues of solution remained on the substrate, leading to a greatly inhomogeneous distribution of PS spheres on the substrate after drying. Again, the samples were dried for 30 minutes at 80°C after the point where no residual solvent could be observed on the substrate by eye. However, all the resulting samples did not meet the requirements stated above. In the literature, very slow coating speeds (down to 1 μm/s) were reported to yield uniform results; but still, with the parameters and system applied by Yang & Jiang[17], monolayer coverage could not be achieved (a minimum of 12 layers of PS spheres were reported).

For all the previously described methods, the substrate plays an important role as the monolayer is assembled directly on its surface. For both silicon wafers (for test/investigative

purposes) and PEN substrates (for the final devices) to be coated equally, the method described in the following seemed to be more suitable: namely, the assembly of a monolayer of polystyrene spheres at the air-water interface and subsequent pick-up on any desired substrate. Furthermore, large areas (tens of cm^2) were reported to be readily coverable by monolayers of PS nanospheres of different sizes with little effort (no need for special equipment).[7] An experimental routine similar to the one reported by Vogel et al.[7] was adopted. First, the commercially available dispersions from Polysciences, Inc. and Microparticles GmbH were each mixed with ethanol (1:1 in volume). A glass beaker (8 cm diameter, 4.5 cm height) was half filled with deionized water and a plasma-cleaned microscopy glass slide (diamond glass) was partially immersed at a tilt angle of ~45°. Drops (microliters in volume) of the PS:H_2O:EtOH solution were added to the dry side of the glass slide above the water. The liquid flowed towards the water surface, where the PS spheres spread immediately. However, with the commercially available spheres tested, no monolayer could be observed on the surface of the water. Immediately after addition of the spheres to the water, the solution turned blurry, indicating the sinking of the spheres below the surface. Changing the amount of ethanol in the suspension with the PS beads was reported to aid spreading of the colloids at the air-water interface.[6] Also the pH of the subphase in the beaker was altered by adding specific amounts of acetic acid (~pH 2.5) or sodium hydroxide (~pH 12). Especially for functionalized colloids, increasing the pH was reported to aid ordering of the resulting monolayers.[7] However, neither of these approaches aided the formation of a monolayer in case of the commercially available beads used. Rey et al.[6] report that part of the reason for such a behavior are impurities and different chemical residues (e.g., initiator) altering the properties of the suspension and the surface of the commercially available colloids, mainly being a consequence of the preparation/polymerization process. Cleaning the beads by multiple centrifugation steps can help to get rid of some impurities; in case of the beads from Polysciences, Inc., Rey et al.[6] reported that even such a procedure did not aid in yielding monolayers of a satisfactory quality.

On the contrary, as described by Vogel et al.[7], the PS spheres obtained by initiator-free emulsion polymerization (provided by Prof. Vogel's group) formed a monolayer readily after adding drops of the corresponding solution to the air-water interface in the described way. Due to the different preparation method, these colloidal solutions exhibit less impurities interfering with the formation of a monolayer on the air-water interface.[6] After adding several drops, a closed monolayer was formed, visible as a continuous interference pattern covering the entire surface of the water (i.e., different colors visible at different angles of incidence).

The transfer of this monolayer onto plasma-cleaned PEN substrates and silicon wafers was performed by taking the substrate with tweezers, immersing it into the water, moving it to an area at which an unaltered monolayer can be seen and picking it up slowly at shallow angles with respect to the water surface. Plasma-cleaning was crucial for the PEN substrates, for without it, no pick-up of large monolayers (areas of cm^2) was possible. The silicon wafers could be used with and without pre-cleaning them by the plasma treatment described. The results on a piece of PEN (a) and on a piece of a silicon wafer (b) are shown in the images in Figure 3.

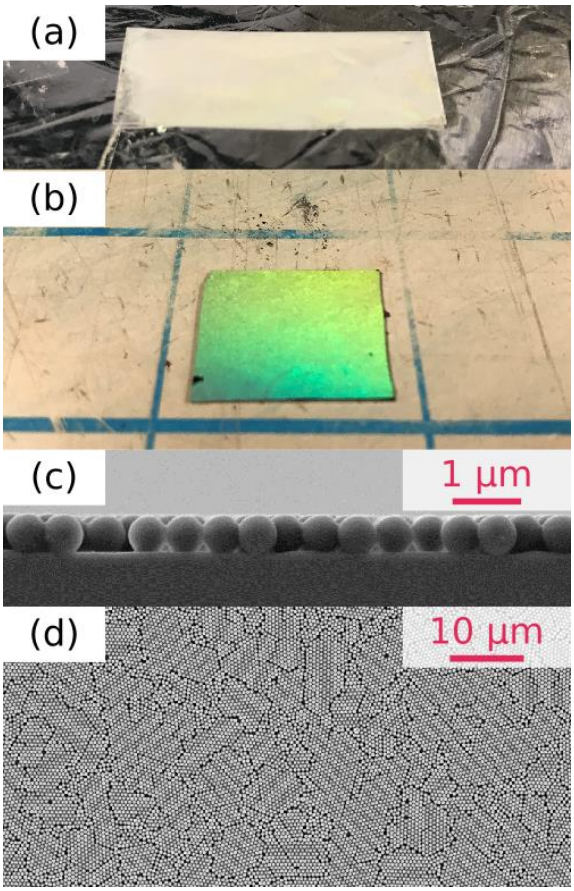

Figure 3: Pictures of a ~3x1 cm piece of PEN (a) and a ~2x2 piece of silicon wafer (b) covered by monolayers of PS spheres (580 nm in diameter) via pick-up after assembly at the air-water interface; side (c) and top view (d) image of a corresponding sample recorded by SEM (on silicon substrate).

The structure of monolayers deposited in such a way is shown in the SEM images in Figure 3 (c) and (d). Almost no double-layer formation/spheres on top of the monolayer were observed. The crystallite size of hexagonal close-packing within the monolayer (defect-free) is in the order of 20x20 spheres. As shown by Rey et al.[6], this value can be greatly increased by cleaning the beads (i.e., centrifuging), fine-tuning the ethanol content in the solution of

the PS beads or changing the pH of the subphase used for the assembly of the colloids in the beaker. In the present project, a process yielding reproducible monolayer coverage with a comparable structure was sufficient. Thus, further efforts for tuning the structure and amount of defects of the monolayers were not pursued.

PEDOT thin film deposition by oCVD

In the second step, the deposition of PEDOT films by oxidative chemical vapor deposition (oCVD) was investigated for the task in question. Since a conformal deposition around 3D-nanostructures is needed, the reactions were run with $VOCl_3$ as the oxidant. $VOCl_3$ is liquid at room temperature and exhibits a vapor pressure high enough in the pressure conditions applied in oCVD for sufficient flow to the reaction chamber. The high volatility of $VOCl_3$ yields a low sticking coefficient and, thus, ensures a high conformality for the resulting coatings.[18] Only few, recent (2019) publications on the deposition of PEDOT films by oCVD with liquid oxidants are available (e.g., with $VOCl_3$ in Gleason's group[19], with $SbCl_5$ and $VOCl_3$ in Nejati's group[10]).

In the beginning, suitable reaction conditions were determined. Overall, the following parameters were varied in order to optimize the depositions in terms of properties of the resulting thin films (as discussed in the further parts of this report): 100-400 mTorr in working pressure, 40-80 °C in substrate temperature and deposition times of 30 or 60 min were adopted. The maximum flow rate of the monomer of 1 sccm (heated to 90°C) achievable with the setup at hand was kept constant for all the depositions. Correspondingly, an equal flow rate of 1 sccm for the oxidant was adopted (also in all depositions) to avoid over-oxidization as reported by Kaviani et al.[10]. The resulting thin films were characterized by Fourier-transform infrared spectroscopy (FTIR). All the spectra recorded on the different samples showed almost identical patterns in terms of peak positions and relative intensities. The absence of a peak at 754 cm^{-1} (attributed to C_α-H) confirms the successful polymerization of EDOT into its polymeric form (PEDOT) during thin film deposition; the FTIR spectra of all the deposited films are in good agreement with data on PEDOT thin films deposited by oCVD with the same oxidant in the literature[10]. This confirms the successful polymerization for all the reaction conditions applied in the present work. Besides the work of Gleason's[19] and Nejati's[10] groups, the present contribution is one of the first reporting on the successful deposition of PEDOT thin films with $VOCl_3$ as the oxidant. Furthermore, the successful deposition of PEDOT thin films onto/around PS nanospheres was confirmed by measuring and comparing FTIR spectra recorded on samples with only PEDOT, only a PS monolayer and with both the

PEDOT and the PS layer on top of each other (see Figure 4); the individual absorption spectra recorded on a monolayer of PS nanospheres and on a PEDOT thin film add up and, thus, can be used to explain all the peaks in the absorption spectrum of a PEDOT thin film deposited onto/around a monolayer of PS nanospheres. A detailed list of peaks assigned to the corresponding molecular vibrations in the structure of PEDOT can be found in the supplementary information to the publication of Kaviani et al.[10]. Accordingly, three main peaks in the spectra of PEDOT recorded within the present work (cf. Figure 4) can be assigned to C-O-C stretching and occur around 1100 cm^{-1} (1090, 1135, 1180 cm^{-1}, respectively).[10] Moreover, C-S-C stretching vibrations can be observed between 650 and 1000 cm^{-1} (685, 825, 970 cm^{-1}, respectively).[10] Peaks at 920 and 1050 cm^{-1} can be assigned to C-S and C-O stretching, respectively, whereas C-C inter-ring stretching bands can be observed at 1320 cm^{-1}.[10]

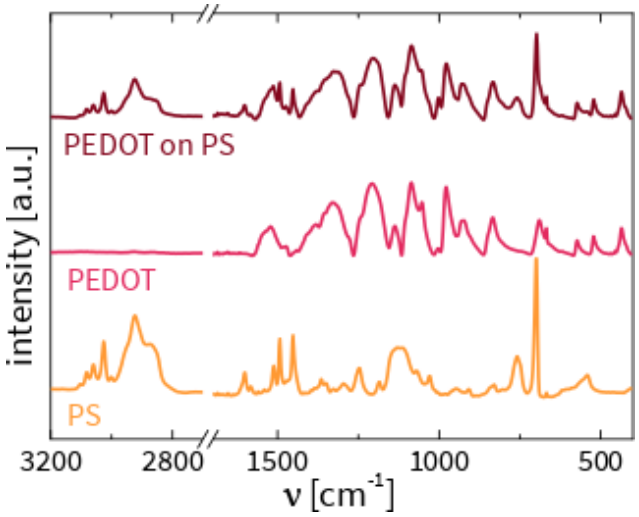

Figure 4: Absorption spectra recorded by FTIR on a PEDOT thin film, a monolayer of PS nanospheres and a PEDOT film deposited onto/around a monolayer of the nanospheres (on silicon substrates).

An estimation of the film thickness of the PEDOT layers resulting from oCVD was performed by SEM of the thin film cross-sections exposed by cleavage of PEDOT-coated silicon substrates after deposition (see Figure 5 (a)). However, especially thin layers (below 100 nm) were at the limit of detection for the SEM used, with charging (visible as a white shroud in Figure 5 (a) at the top of the thin film) and lack of contrast blurring the images. However, the film thickness of thinner layers could be estimated by assuming constant deposition rate over time and back-calculating from the longer depositions. All the layers investigated exhibited thickness values between 50 nm and 1 µm, with lower pressure, higher substrate temperature and shorter reaction time leading to thinner films, as expected in most CVD processes. However, film

thickness was not the most crucial parameter, as the main aim was to deposit uniform and conformal PEDOT layers onto/around PS nanospheres. Regardless, SEM helped to identify the most promising deposition conditions and resulting structures. The fastest depositions (i.e., highest working pressure) developed cracks when taking them out of the reactor, hinting towards a substantial strain in the films deposited in such a manner. Regardless, slower depositions yielded thin film samples with excellent uniformity, without the presence of any appreciable observable defects (cf. Figure 5 (a)).

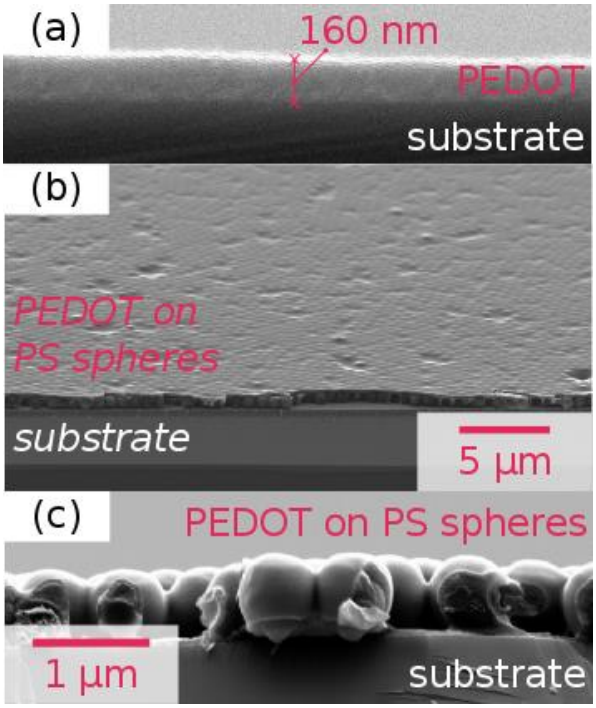

Figure 5: Representative SEM images of (a) a 160-nm-thick PEDOT thin film on a silicon substrate (side view), (b) a PEDOT film deposited onto/around PS nanospheres (angled view) and (c) a close-up image (side view) of a sample with a thin PEDOT layer deposited onto/around PS nanospheres to demonstrate the conformality of the deposition.

For the deposition onto substrates pre-covered by a monolayer of PS nanospheres, the following results can be summarized: the most conformal depositions around the PS nanostructures were achieved at relatively low pressures (i.e., slow depositions). For thicker depositions (>100 nm), a flat PEDOT layer on top of the nanostructures was observed to form, covering all the nanostructures. The thicker this top layer was, the less structured the film's surface looked from the top due to smoothening by the deposited PEDOT film with increasing deposited thickness.

The threshold in thickness observed (~100 nm) coincides with the thickness needed to be deposited for complete filling of the voids of the hcp-structure between the flat substrate surface and the nanospheres. From geometrical considerations, the point last filled by a conformal and constant growth both from the substrate and the nanosphere surfaces can be estimated (see Figure 6). Geometrically, this point must lie equidistant between the surfaces of the three surrounding spheres and the substrate surface. Therefore, as evident from a projection from top or bottom (see Figure 6 (b)), this point has to lie exactly on the line perpendicular to the substrate that passes through the center of the triangle formed by the centers of the three surrounding spheres (marked as an orange line in (a) and an orange x in (b) of Figure 6). The distance d_{sph} of each point on this line relative (perpendicular) to the surface of one of the spheres with radius r can be written as a function of the angle φ from the plane formed by the centers of the surrounding spheres, which reads as follows:

$$d_{sph} = r\,(\frac{2}{\sqrt{3}\cos\varphi} - 1)$$

The distance d_{sub} on this line from the substrate surface can be written as a function of the same angle φ as follows:

$$d_{sub} = r\,(1 - \frac{2\tan\varphi}{\sqrt{3}})$$

By equating the distances from the surface of one of the spheres (d_{sph}) and from the substrate surface (d_{sub}), the exact thickness t can be calculated, at which a conformal and equal growth from all the surrounding surfaces would meet last. Solving for the angle φ in the first quadrant yields $\varphi = \pi/6$. Inserting this value into one of the equations for d_{sph} or d_{sub} with r = (580 nm/2) yields $t \approx 97$ nm. However, when including the fact that new molecules for film growth need to arrive at each spot on the surface from top, the path is blocked earlier; this happens exactly, when the smallest voids between the spheres (i.e., at half the height of the spheres) are closed. This point in thickness can be estimated by calculating the distance between the surface of a sphere at half the height of the sphere to the center of the triangle formed by the three centers of the surrounding spheres (see Figure 6 (b)); it is visualized as the line labelled s in green. For spheres with a diameter of 580 nm, $s \approx 45$ nm. Furthermore, the fact that the growth is not perfectly conformal and effects such as capillary condensation, altering the growth in small voids, need to be considered. In the present work, we aim at minimizing the growth of PEDOT in a flat layer above the PS nanospheres because the interfaces between PEDOT and PSS were reported to play an important role in the piezoresistive behavior. Therefore, slow

depositions (i.e., low working pressure of 200 mTorr) between 50 and 100 nm in thickness (on a flat silicon substrate) were evaluated to yield the most promising results on the nanospheres by SEM (also in terms of uniformity (b) and conformality (c); see Figure 5). Therefore, these conditions were adopted for the depositions on the PS spheres for the further device fabrication. Overall, this contribution is among the first to report on the conformal and uniform oCVD of conducting polymer thin films around nanospheres.

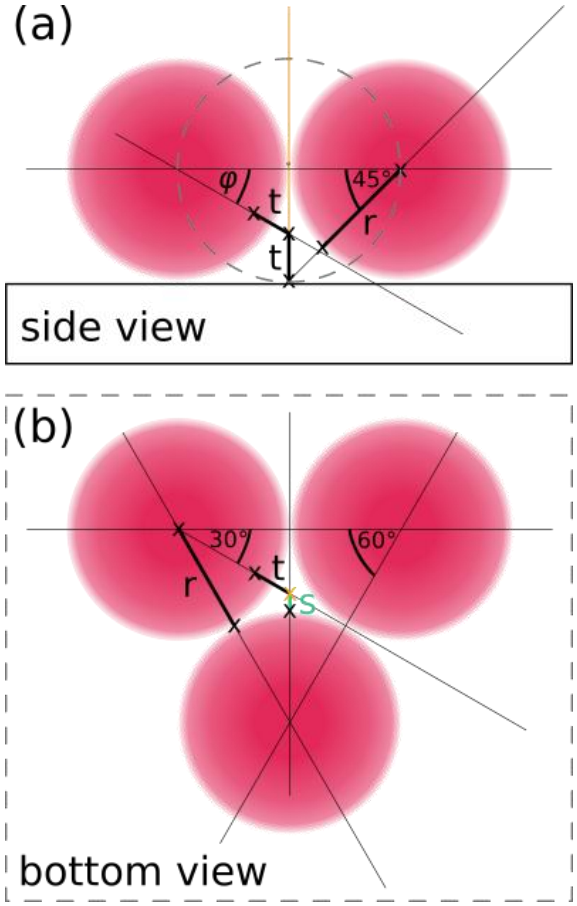

Figure 6: Side view (a) and bottom view (b) sketches of 2D-projections of parts of the hcp-structure of nanospheres (with radius *r*) on a substrate surface aiding to explain the geometrical considerations behind the estimation of the point (at thickness *t*) last filled by a conformal growth of a film on the substrate and the nanosphere surfaces; dashed lines give shapes that need to be seen through to observe the sketched structures (nanosphere in (a) and substrate in (b)).

Regarding deposition conditions influencing material properties possibly altering the electrical and piezoresistive properties of the resulting thin films, the conductivity of oCVD-PEDOT films was reported to increase with increased substrate temperature during deposition.[10] To not damage the PS spheres thermally (i.e., glass transition temperature of

polystyrene at ~100-107 °C)[20], substrate temperatures of 60 and 80 °C were applied for the deposition of PEDOT on the nanospheres. The two temperatures were also chosen to investigate the effect of the conductivity on the piezoresistive properties of the samples.

Assembly and testing of devices

For the fabrication of the actual piezoresistive devices, a monolayer of PS nanospheres was deposited onto PEN substrates (3x1 cm) via pick-up of the monolayer assembled at the air-water interface. Subsequently, PEDOT thin films were deposited onto the nanospheres at different substrate temperatures and thicknesses. Various samples were acid-treated by placing them in a 0.5 M H_2SO_4 solution for 10 min. This procedure is performed to achieve a dopant exchange process in the PEDOT layer such as described by Howden et al.[8] and a sulfonation of the surfaces of the PS spheres as reported by Nucara et al.[9]. Two 50-nm-thick nickel contacts were evaporated onto the PEDOT via physical vapor deposition (PVD). The two contacts were prepared with a separation of 0.5 mm via masking during deposition. Nickel was chosen due to its work function (4.9-5.2 eV in films)[21], matching the estimated work function of PEDOT (5.1-5.2 eV in oCVD films)[22], yielding ohmic behavior. The piezoresistive properties of these samples were investigated by determining their resistance as a function of straining. Initially, voltage-current measurements (see Figure 7) were performed. All samples showed straight voltage-current characteristics, confirming the ohmic behavior of the devices (with nickel contacts). For the sake of usability, further measurements of the resistance were performed directly with a multimeter.

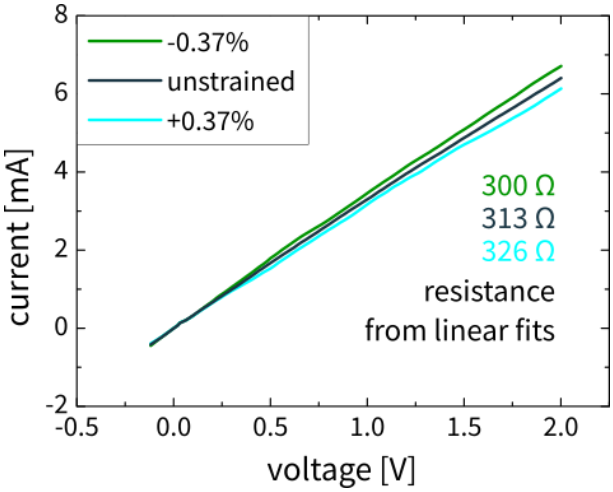

Figure 7: Representative voltage-current characteristics (from -0.1 to 2 V) measured on a strained and unstrained device structure with the respective resistance values calculated from linear fits of the curves (reciprocal value of the slope); preparation conditions: T_{sub} = 80 °C, 60 min, H_2SO_4-treated.

The resistance values of the unstrained devices (as-deposited and with 10 min H_2SO_4-treatment) measured directly with a multimeter are given in Table 1. In accordance with literature (e.g., Kaviani et al.[10]), the conductivity appears to increase with substrate temperature and with deposited film thickness (i.e., deposition time), observable as a decreased resistance value. Furthermore, H_2SO_4-treatment decreases the resistance by ~1/3. For PEDOT films deposited with iron chloride as the oxidant, even larger increases in conductivity were observed (more than 100%), possibly due to different species and levels of doping. However, the present work is among or even the first to report on a dopant exchange in sulfuric acid enhancing the conductivity of oCVD-PEDOT films deposited with $VOCl_3$ as the oxidant by ~1/3.

The H_2SO_4-treated sample deposited at 80 °C substrate temperature with a deposition time of 60 minutes (cf. Figure 7) shows a slightly lower resistance value when calculated from the slope of the voltage-current characteristics (~313 Ω) compared to the value obtained from a direct measurement with the multimeter (cf. Table 1; 298 Ω) in its unstrained state. The measurement uncertainty and different wire and contact probe resistances might be possible sources for this difference. All the differences between the resistance values obtained from voltage-current characteristics and direct measurement lie within this range. For the remaining results of this contribution, the direct measurements are reported due to their ease in measurement (especially during bending). Regardless, both sets of data show the same trends.

Table 1: Resistance measured on device structures as-deposited and after 10 min of H_2SO_4-treatment for different deposition conditions

	Resistance [Ω]	
Deposition conditions	as-deposited	H_2SO_4-treated
60 °C;30 min	1,711 ± 16	1,056 ± 11
60 °C;60 min	448 ± 6	320 ± 5
80 °C;30 min	1059 ± 11	717 ± 7
80 °C;60 min	397 ± 6	298 ± 5

With the geometry of the samples, their conductivity can be estimated to range in values of up to tens of S cm^{-1}, which is in the range of conductivity values reported in other studies on

oCVD-PEDOT[15] and especially on films deposited at relatively low substrate temperatures.[10] For depositions carried out at even higher substrate temperatures (e.g., 145°C), conductivity values of up to several thousands of S cm^{-1} were reported.[10,19] Regarding the response to bending, Figure 7 gives an idea about the amplitude of the change in resistance (~4% for an applied strain of 0.37% for the respective sample). Compressive and tensile strain yield shifts in the opposite direction but comparable in magnitude. A summary of the response of the different samples to 0.37% of tensile strain is given in Table 2.

Table 2: Response in change of resistance (percent compared to the unstrained state) to 0.37% of tensile strain (applied via bending) measured on device structures as-deposited and after 10 min of H_2SO_4-treatment for different deposition conditions

	Response [%]	
Deposition conditions	as-deposited	H_2SO_4-treated
60 °C;30 min	0.2	0.4
60 °C;60 min	0.5	0.9
80 °C;30 min	0.8	1.6
80 °C;60 min	2.3	4.2

The data in Table 2 shows that the response to 0.37% of tensile strain (applied via bending) is higher for samples prepared at higher substrate temperature (i.e., more conductive) and longer deposition time (i.e., greater deposited film thickness). Furthermore, an increase of the response by a factor of ~2 is observed after acid treatment, indicating an influence of the dopant species on the piezoresistive behavior. Howden et al.[8] hypothesize that acid rinsing has multiple potential effects on such vapor-deposited PEDOT films: It could help in removing residual oxidant from the film, in solvating the structure to allow for optimized morphology and in lowering the film roughness. Furthermore, the solvating effect was expected to allow for the incorporation of further dopant ions, observable in a higher doping level and, thus, conductivity.[8] Furthermore, the sulfonated PEDOT-PSS interfaces are expected to contribute to the enhanced piezoresistive response, as reported and hypothesized in the literature on PEDOT:PSS-based piezoresistive devices.[3,4,23] Overall, a correlation between an increase in conductivity and an increase in gauge factor were found in the investigated samples.

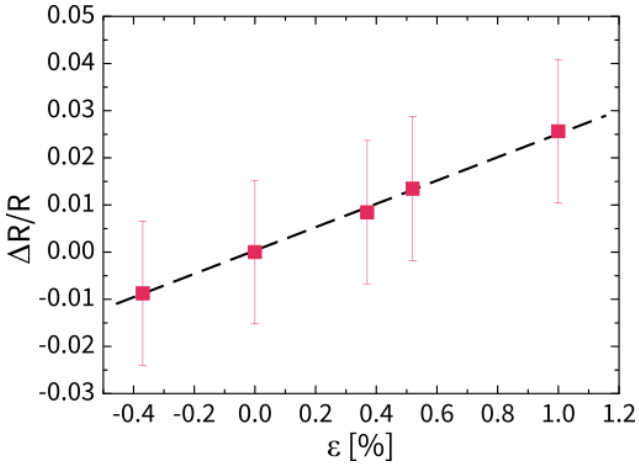

Figure 8: Representative data on the change in resistance normalized by the resistance of the unstrained device (ΔR/R) as a function of strain ε (in percent); preparation conditions: T_{sub} = 60 °C, 60 min, H_2SO_4-treated; the dashed line represents a linear fit to the measurement points

With bending, different levels of strain (i.e., bending radii) can be applied on the devices. From such experiments (see Figure 8), the relation between the change in resistance and the applied strain can be investigated. Successful fitting of the measured data with a linear function leads to the hypothesis of a linear relationship between these two parameters in the range of strains investigated. The uncertainties for the measured resistance values (cf. error bars in Figure 8) arise from the measurement uncertainty of the multimeter. Despite the large uncertainty, as it is close to being constant for all the data points plotted, the linearity of the relation described can be assumed to be valid. Moreover, this relationship is confirmed by voltage-current measurements and by all the samples investigated in the present study exhibiting a similar relationship. This behavior is expected and reported widely in the literature.[2,3]

Furthermore, this relation is widely used to estimate the quality of a piezoresistive device. The quantity measuring this correlation is called gauge factor k. It relates the measured resistance change normalized by the resistance of the unstrained device ($\Delta R/R$) to the applied strain ε as the change in length normalized by the length in the unstrained state ($\Delta l/l$) as follows:

$$k = \frac{(\Delta R/R)}{(\Delta l/l)} = \frac{(\Delta R/R)}{\varepsilon}$$

Thus, with the values from Table 2, the gauge factors can be calculated, yielding values of as high as 11.4. Furthermore, the Poisson's ratio of the polymer (ν), describing the transverse

change in length resulting from longitudinal straining, can be estimated to be ~0.35.[2] This can be used to subtract the factor merely resulting from the geometrical change upon straining the device as follows:[1]

$$k = 1 + 2\nu + \frac{1}{\varepsilon}\frac{\Delta\rho}{\rho} = 1 + 2\nu + k_\rho$$

This yields an estimation of ~9.7 to be the value for the corresponding "true" gauge factor (k_ρ) resulting from the change in conductivity (ρ) of the polymeric structure. Still, this value lies well above gauge factors of conventional metal strain gauges (k<5).[1] Considering the values of other polymer-based materials, the measured k value compares well to gauge factors determined on PEDOT:PSS-based structures measured in similar configurations (e.g., 0.48,[2] 17.8[3]). In conventional semiconductors (e.g., silicon, germanium), gauge factors of >100 have been reported.[24] However, these materials bear the disadvantage of a trade-off between their rigidity connected to the disability to sense large strains and/or small pressures and a high gauge factor. Furthermore, in a more sophisticated sandwich geometry (top-bottom contacting), very large responses to pressure (changes of the resistance of up to ~3 orders of magnitude) were reported for PEDOT:PSS films containing gold nanoparticles.[4] However, these devices exhibited a very large intrinsic resistance in their unstrained state (~10^{11} Ω). Furthermore, very high gauge factors (55-396), depending on the range of strains applied, were reported for an electrospun PEDOT:PSS-PVA nanofiber material; also for this material, low conductivities were reported (10^{-5}-10^{-8} Scm^{-1}).[5]

Regardless, it should be mentioned that the magnitude of the gauge factor is not the only parameter relevant for piezoresistive devices. For instance, the mechanical flexibility, elasticity, compatibility with biological systems and low-cost of fully polymeric setups makes them particularly interesting for future applications. Thus, structures like the proposed one here show great potential and exhibit a set of properties that is crucial for various different applications such as in biosystems or wearable electronics.

In the present work, a simple approach for testing a novel set of materials was adopted. It must be mentioned that the results published in this work should be regarded as preliminary. Herein, the materials and the measurement geometry have not been optimized to their full potential. For instance, different read-out geometries (e.g., sandwich) could be promising approaches. Optimizing the set of materials and structures used yields further opportunities of improving device performance. On the one hand, the possibility of changing the size of the polystyrene nanospheres represents a knob to tune the interfacial contact area between

PEDOT and PS(S). On the other hand, especially, the oCVD process yields great potential of tailoring and tuning material properties of the PEDOT layer such as conductivity and conjugation length,[10,19] directly influencing the piezoresistive behavior of the resulting material. As an increased conductivity was found to correlate with an increased gauge factor, a very promising outlook are the remarkably high conductivity values (thousands of S cm^{-1}) reported on oCVD PEDOT in the literature.[10,19] Besides substrate temperature and film thickness, the working pressure and the nature and flow rates of the individual chemicals used within the process were shown to alter the microstructure and the material properties of the resulting thin films further.[11,19] As the conductivity of the PEDOT film depends on doping, the oxidant species used within the oCVD process may be an interesting knob to play with (e.g., $SbCl_5$ as used by Nejati's group[10]). Moreover, the acid treatment (e.g., different acids) can be used to alter the resulting chemical nature of doping. Compared to regular PEDOT:PSS-based structures, the methods applied in the present work open up a vast number of tunable parameters, potentially enabling the structures to outperform conventional architectures. Moreover, the reported results broaden the impact and possibilities of applications of oCVD films.

Conclusions

In this work, a novel, fully polymeric composite material for piezoresistive devices was proposed, prepared and tested. The deposition of a monolayer of polystyrene nanospheres onto flexible polyethylene naphthalate (PEN) substrates over large areas (several cm^2) was achieved by the assembly of the monolayer at the air-water interface and subsequent pick-up with the plasma-cleaned PEN substrates. A thin layer (~50-100 nm) of PEDOT was deposited conformally around the PS nanospheres via oxidative chemical vapor deposition (oCVD). The successful polymerization and deposition were confirmed by scanning electron microscopy and Fourier-transform infrared spectroscopy. The intrinsically chlorine-doped nature of the oCVD-PEDOT layers was altered by a treatment in sulfuric acid post deposition. During deposition of the PEDOT thin film, the substrate temperature and deposited thickness were used as parameters to alter film properties in terms of conductivity and piezoresistive response.

Two nickel top-contacts were evaporated on top of the assembled PEN/PS/PEDOT-structure with a separation of 0.5 mm to allow for the electric characterization of the individual samples. The ohmic nature of the contacts and the entire device structure were confirmed by the linearity of their voltage-current characteristics (also when strained). Resistance measurements revealed that preparing the samples at higher substrate temperature and increasing the deposited thickness yield structures exhibiting lower resistance. The dopant exchange performed by acid treatment in sulfuric acid decreased the samples' resistance by ~1/3. Conductivities were estimated to range as high as tens of S cm^{-1}. To test the piezoresistive properties of the samples, resistance measurements during defined bending (i.e., strain) were performed. All samples prepared were confirmed to exhibit piezoresistive behavior by changing their resistance as a function of applied strain. Lower intrinsic resistance (i.e., samples prepared at higher substrate temperature, samples with increased thickness) enhanced the piezoresistive response of the samples. Furthermore, the acid treatment applied increased the piezoresistive response of the samples by a factor of ~2. Besides performing dopant exchange, additional doping and optimizing the morphology of/in the PEDOT layer, this treatment is thought to sulfonate the surfaces of the PS spheres, contributing to the piezoresistive behavior of the final devices. From the relationship of the applied strain to the change in resistance measured, gauge factors as high as 11.4 were determined.

Overall, the results presented in this contribution serve as a promising basis for the optimization and development of the investigated structures for their application in piezoresistive devices. Further investigation on the performance of the proposed structures are needed and an optimized setup for the application of the investigated architectures is sought. Regardless, already the combination and substeps of the methods applied yielded novel insights into the capabilities of the investigated systems.

Abbreviations used

oCVD	oxidative Chemical Vapor Deposition
hcp	hexagonally close-packed
PS	polystyrene
PSS	polystyrene sulfonate
PEDOT	poly(3,4-ethylenedioxythiophene)
PEN	polyethylene naphthalate
MeOH, EtOH	methanol, ethanol
SEM	scanning electron microscopy
FTIR	Fourier-transform infrared spectroscopy

References

(1) Fiorillo, A. S.; Critello, C. D.; Pullano, A. S. Theory, Technology and Applications of Piezoresistive Sensors: A Review. *Sensors Actuators, A Phys.* **2018**, *281*, 156–175. https://doi.org/10.1016/j.sna.2018.07.006.

(2) Lang, U.; Rust, P.; Schoberle, B.; Dual, J. Piezoresistive Properties of PEDOT:PSS. *Microelectron. Eng.* **2009**, *86* (3), 330–334. https://doi.org/10.1016/j.mee.2008.10.024.

(3) Latessa, G.; Brunetti, F.; Reale, A.; Saggio, G.; Di Carlo, A. Piezoresistive Behaviour of Flexible PEDOT:PSS Based Sensors. *Sensors Actuators, B Chem.* **2009**, *139* (2), 304–309. https://doi.org/10.1016/j.snb.2009.03.063.

(4) Karmakar, R. S.; Lu, Y. J.; Fu, Y.; Wei, K. C.; Chan, S. H.; Wu, M. C.; Lee, J. W.; Lin, T. K.; Wang, J. C. Cross-Talk Immunity of PEDOT:PSS Pressure Sensing Arrays with Gold Nanoparticle Incorporation. *Sci. Rep.* **2017**, *7*, 12252. https://doi.org/10.1038/s41598-017-12420-5.

(5) Liu, N.; Fang, G.; Wan, J.; Zhou, H.; Long, H.; Zhao, X. Electrospun PEDOT:PSS-PVA Nanofiber Based Ultrahigh-Strain Sensors with Controllable Electrical Conductivity. *J. Mater. Chem.* **2011**, *21*, 18962–18966. https://doi.org/10.1039/c1jm14491j.

(6) Rey, M.; Yu, T.; Guenther, R.; Bley, K.; Vogel, N. A Dirty Story: Improving Colloidal Monolayer Formation by Understanding the Effect of Impurities at the Air/Water Interface. *Langmuir* **2019**, *35* (1), 95–103. https://doi.org/10.1021/acs.langmuir.8b02605.

(7) Vogel, N.; Goerres, S.; Landfester, K.; Weiss, C. K. A Convenient Method to Produce Close- and Non-Close-Packed Monolayers Using Direct Assembly at the Air-Water Interface and Subsequent Plasma-Induced Size Reduction. *Macromol. Chem. Phys.* **2011**, *212* (16), 1719–1734. https://doi.org/10.1002/macp.201100187.

(8) Howden, R. M.; McVay, E. D.; Gleason, K. K. OCVD Poly(3,4-Ethylenedioxythiophene) Conductivity and Lifetime Enhancement via Acid Rinse Dopant Exchange. *J. Mater. Chem. A* **2013**, *1*, 1334–1340. https://doi.org/10.1039/c2ta00321j.

(9) Nucara, L.; Piazza, V.; Greco, F.; Robbiano, V.; Cappello, V.; Gemmi, M.; Cacialli, F.; Mattoli, V. Ionic Strength Responsive Sulfonated Polystyrene Opals. *ACS Appl. Mater. Interfaces* **2017**, *9* (5), 4818–4827. https://doi.org/10.1021/acsami.6b14455.

(10) Kaviani, S.; Mohammadi Ghaleni, M.; Tavakoli, E.; Nejati, S. Electroactive and Conformal Coatings of Oxidative Chemical Vapor Deposition Polymers for Oxygen Electroreduction. *ACS Appl. Polym. Mater.* **2019**, *1* (3), 552–560. https://doi.org/10.1021/acsapm.8b00240.

(11) Smolin, Y. Y.; Soroush, M.; Lau, K. K. S. Oxidative Chemical Vapor Deposition of Polyaniline Thin Films. *Beilstein J. Nanotechnol.* **2017**, *4* (8), 1601201. https://doi.org/10.3762/bjnano.8.128.

(12) Smolin, Y. Y.; Soroush, M.; Lau, K. K. S. Influence of OCVD Polyaniline Film Chemistry in Carbon-Based Supercapacitors. *Ind. Eng. Chem. Res.* **2017**, *56* (21), 6221–6228. https://doi.org/10.1021/acs.iecr.7b00441.

(13) Hulteen, J. C.; Treichel, D. A.; Smith, M. T.; Duval, M. L.; Jensen, T. R.; Van Duyne, R. P. Nanosphere Lithography: Size-Tunable Silver Nanoparticle and Surface Cluster Arrays. *J. Phys. Chem. B* **1999**, *103* (19), 3854–3863. https://doi.org/10.1021/jp9904771.

(14) Trujillo, N. J.; Baxamusa, S. H.; Gleason, K. K. Grafted Functional Polymer Nanostructures Patterned Bottom-up by Colloidal Lithography and Initiated Chemical Vapor Deposition (ICVD). *Chem. Mater.* **2009**, *21* (4), 742–750. https://doi.org/10.1021/cm803008r.

(15) Trujillo, N. J.; Barr, M. C.; Im, S. G.; Gleason, K. K. Oxidative Chemical Vapor Deposition (OCVD) of Patterned and Functional Grafted Conducting Polymer Nanostructures. *J. Mater. Chem.* **2010**. https://doi.org/10.1039/b925736e.

(16) Arutinov, G.; Brichkin, S. B.; Razumov, V. F. Self-Assembling of Polystyrene Microsphere Monolayers by Spin-Coating. *Nanotechnologies Russ.* **2010**. https://doi.org/10.1134/S1995078010010064.

(17) Yang, H.; Jiang, P. Large-Scale Colloidal Self-Assembly by Doctor Blade Coating. *Langmuir* **2010**, *26* (16), 13173–13182. https://doi.org/10.1021/la101721v.

(18) Chelawat, H.; Vaddiraju, S.; Gleason, K. Conformal, Conducting Poly(3,4-Ethylenedioxythiophene) Thin Films Deposited Using Bromine as the Oxidant in a Completely Dry Oxidative Chemical Vapor Deposition Process. *Chem. Mater.* **2010**, *22* (9), 2864–2868. https://doi.org/10.1021/cm100092c.

(19) Gharahcheshmeh, M. H.; Tavakoli, M. M.; Gleason, E. F.; Robinson, M. T.; Kong, J.; Gleason, K. K. Tuning, Optimization, and Perovskite Solar Cell Device Integration of Ultrathin Poly(3,4-Ethylene Dioxythiophene) Films via a Single-Step All-Dry Process. *Sci. Adv.* **2019**, *5* (11), eaay0414. https://doi.org/10.1126/sciadv.aay0414.

(20) Rieger, J. The Glass Transition Temperature of Polystyrene. *J. Therm. Anal.* **1996**, *46*, 965–972. https://doi.org/10.1007/bf01983614.

(21) Baker, B. G.; Johnson, B. B.; Maire, G. L. C. Photoelectric Work Function Measurements on Nickel Crystals and Films. *Surf. Sci.* **1971**, *24* (2), 572–586. https://doi.org/10.1016/0039-6028(71)90282-2.

(22) Im, S. G.; Gleason, K. K.; Olivetti, E. A. Doping Level and Work Function Control in Oxidative Chemical Vapor Deposited Poly (3,4-Ethylenedioxythiophene). *Appl. Phys. Lett.* **2007**, *90*, 152112. https://doi.org/10.1063/1.2721376.

(23) Wang, J. C.; Wang, J. C.; Subhra Karmakar, R.; Lu, Y. J.; Huang, C. Y.; Wei, K. C. Characterization of Piezoresistive PEDOT:PSS Pressure Sensors with Inter-Digitated and Cross-Point Electrode Structures. *Sensors* **2015**, *15* (1), 818–831. https://doi.org/10.3390/s150100818.

(24) Yang, S.; Lu, N. Gauge Factor and Stretchability of Silicon-on-Polymer Strain Gauges. *Sensors* **2013**, *13* (7), 8577–8594. https://doi.org/10.3390/s130708577.